Available online at www.sciencedirect.com
ScienceDirect
Journal of Controlled Release 115 (2006) 344–353
journal of controlled release
www.elsevier.com/locate/jconrel

Erbium:YAG laser-mediated oligonucleotide and DNA delivery via the skin: An animal study

Woan-Ruoh Lee [a,b], Shing-Chuan Shen [c,d], Ching-Ru Liu [e], Chia-Lang Fang [f], Chung-Hong Hu [c,d], Jia-You Fang [e,*]

[a] Department of Dermatology, Taipei Medical University Hospital, Taipei, Taiwan
[b] Graduate Institute of Medical Sciences, Taipei Medical University, Taipei, Taiwan
[c] Department of Dermatology, College of Medicine, Taipei Medical University, Taipei, Taiwan
[d] Department of Dermatology, Taipei Municipal Wan Fang Hospital, Taipei, Taiwan
[e] Pharmaceutics Laboratory, Graduate Institute of Natural Products, Chang Gung University, Kweishan, Taoyuan, Taiwan
[f] Department of Pathology, College of Medicine, Taipei Medical University, Taipei, Taiwan

Received 21 April 2006; accepted 15 August 2006
Available online 23 August 2006

Abstract

Topical delivery of antisense oligonucleotides (ASOs) and DNA is attractive for treatment of skin disorders. However, this delivery method is limited by the low permeability of the stratum corneum (SC). The objective of this study was to enhance and optimize the skin absorption of gene-based drugs by an erbium:yttrium-aluminum-garnet (Er:YAG) laser. The animal model utilized nude mice. In the in vitro permeation study, the Er:YAG laser treatment produced a 3–30-fold increase in ASO permeation which was dependent on the laser fluence and ASO molecular mass used. The fluorescence microscopic images showed a more-significant localization of a 15-mer ASO in the epidermis and hair follicles after laser application as compared with the control. The expressions of reporter genes coding for β-galactosidase and green fluorescent protein (GFP) in skin were assessed by X-gal staining and confocal laser scanning microscopy. The SC ablation effect and photomechanical waves produced by the Er:YAG laser resulted in DNA expression being extensively distributed from the epidermis to the subcutis. The GFP expression in 1.4 J/cm^2-treated skin was 160-fold higher than that in intact skin. This non-invasive, well-controlled technique of using an Er:YAG laser for gene therapy provides an efficient strategy to deliver ASOs and DNA via the skin.

Keywords: Erbium:YAG laser; Oligonucleotide; DNA; Skin; Topical delivery

1. Introduction

Gene therapy is defined as the introduction of an exogenous gene into a host cell to achieve therapeutic benefits. The skin is an attractive target organ for gene therapy because it is readily accessible and can be easily monitored [1,2]. Antisense oligonucleotides (ASOs) are a novel class of therapeutic agents consisting of a short piece of single-stranded DNA that can hybridize and downregulate a target mRNA that encodes a particular protein involved in the development of a certain disease [3]. Topical delivery of ASOs is a promising technique, especially for the treatment of local skin disorders including skin carcinomas, melanomas, psoriasis, inflammation, and herpes simplex [4]. Topical DNA delivery is also being evaluated in many clinical situations in the treatment of cutaneous disorders such as melanomas, skin wounds, wrinkles, and hyperkeratosis [5]. In addition to treating skin diseases, cutaneous ASO and DNA delivery can be used to express gene products with systemic effects [6,7].

Despite all of these benefits of gene therapy via the skin, ASO and DNA delivery is still severely limited by the low permeation of most substances through the stratum corneum (SC). A poor permeability of genes across the skin is predicted because of their physicochemical characteristics such as a high molecular weight, hydrophilic nature, and multiple negative charges [3,8].

* Corresponding author. Pharmaceutics Laboratory, Graduate Institute of Natural Products, Chang Gung University, 259 Wen-Hwa 1st Road, Kweishan, Taoyuan 333, Taiwan. Tel.: +886 3 2118800x5521; fax: +886 3 2118236.
E-mail address: fajy@mail.cgu.edu.tw (J.-Y. Fang).

0168-3659/$ - see front matter © 2006 Elsevier B.V. All rights reserved.
doi:10.1016/j.jconrel.2006.08.012

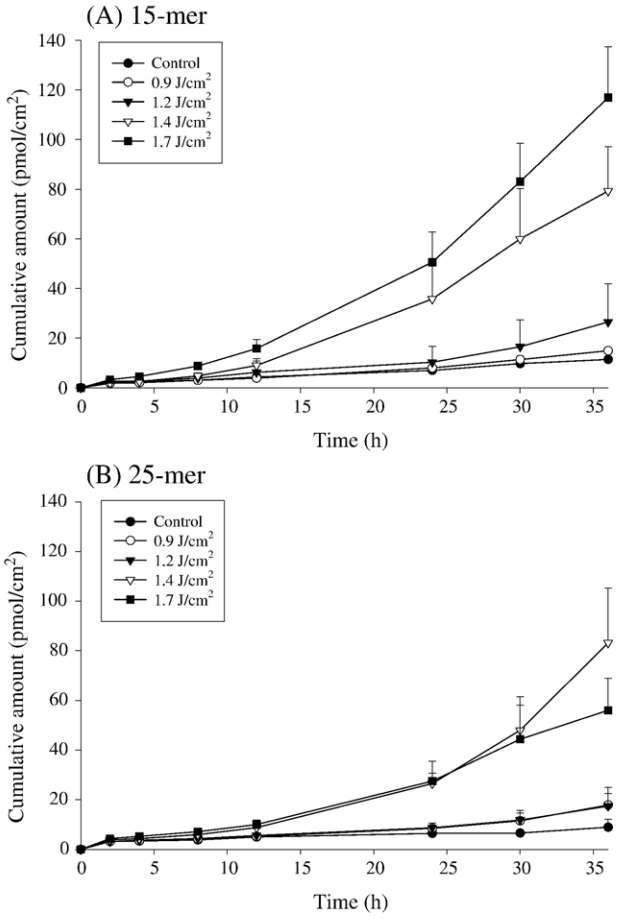

Fig. 1. In vitro cumulative amount-time profiles of topical permeation of an ASO of 15 (A) and 25-mers (B) after Er:YAG laser treatment of skin at various fluences. Each value represents the mean±S.D. (n=4).

Hence gene transfer via the skin has many potential applications but lacks a safe and efficient delivery method. Removal of the SC by mechanical abrasion, tape-stripping, or chemical treatment has been shown to significantly enhance permeation of ASOs and DNA [9]. However, these approaches may be limited due to the lack of control and reproducibility, as well as their potential to cause irritation [10]. We recently suggested that the erbium:yttrium-aluminum-garnet (Er:YAG) laser can effectively enhance and precisely control in vitro drug delivery via the skin, including nalbuphine, 5-fluorouracil, vitamin C, 5-aminolevulinic acid, and dextran [11–15]. The Er:YAG laser is very popular nowadays, because it can ablate the SC with minimal residual thermal damage to the skin. It is currently used for the resurfacing of rhytides, scars, and photodamage.

The aim of the present study was to assess the feasibility of topical ASO and DNA delivery using a pulse of an Er:YAG laser. This study utilized in vitro Franz cells for evaluating the topical delivery of fluorescein-labeled ASOs. In the in vivo study, the distribution of ASOs and the expressions of β-galactosidase and green fluorescent protein (GFP) in nude mouse skin were studied to assess the targeting characteristics of the present gene transfection.

2. Materials and methods

2.1. Materials

The 5′-fluorescein-labeled antisense phosphorothioate oligonucleotides (ASOs) of 15-mers (sequence: 5′-ACCAATCAGA CACCA-3′, molecular weight: 5036 g/mol) and 25-mers (sequence: 5′-ACCAATCAGACACCAACCAATCAGA-3′, molecular weight: 8103 g/mol) were synthesized by MWG Biotech AG Company (Ebersberg, Germany). A 4.7-kb plasmid (pAcGFP1-C1) with a CMV promoter was purchased from BD Biosciences (Palo Alto, CA, USA). The plasmid PCMV-β encoding the *Escherichia coli lac* Z (β-galactosidase) gene expression plasmid (3.0 kb) was kindly provided by Dr. B.C. Chen (Taipei Medical University, Taipei, Taiwan). Sulforhodamine B (SRB) was supplied by Sigma Chemicals (St. Louis, MO, USA). A Maxi-V500 plasmid extraction system was obtained from Viogene (Taipei, Taiwan). A X-gal staining assay kit was purchased from Gene Therapy Systems (San Diego, CA, USA).

2.2. Er:YAG laser assembly

The Er:YAG laser (Continuum Biomedical, Santa Clara, CA, USA) used here has a wavelength of 2940 nm and a pulse duration of 250 μs. An articulated arm was used to deliver the laser beam

Table 1
The fluxes and enhancement ratios of oligonucleotides across nude mouse skin by treatment of Er:YAG laser

Fluence (J/cm^2)	15-mer			25-mer		
	Original flux (pmol/cm^2/h) [a]	Normalized flux (pmol/cm^2/h) [b]	Enhancement ratio (ER) [c]	Original flux (pmol/cm^2/h)	Normalized flux (pmol/cm^2/h)	Enhancement ratio (ER)
0	0.29±0.05	–	–	0.19±0.05	–	–
0.9	0.38±0.15	0.56±0.22	–	0.40±0.17	0.81±0.35	4.3
1.2	0.62±0.29	1.27±0.59	4.4	0.39±0.12	0.78±0.24	4.1
1.4	2.18±0.63	5.91±1.71	20.4	1.99±0.45	5.54±1.25	29.2
1.7	3.11±0.65	8.68±1.81	29.9	1.50±0.40	4.09±1.09	21.5
Tape-stripping	7.32±0.23	7.32±0.23	25.2	5.69±0.52	5.69±0.52	30.0

Each value represents the mean±S.D. (n=4–8).
[a] Original flux was calculated directly from the flux across partly laser-treated skin.
[b] Normalized flux was calculated from the flux across fully laser-treated skin (100%), which was calibrated by flux of control group (without laser treatment).
[c] Enhancement ratio (ER) was normalized flux of laser-treated group/flux of control group.

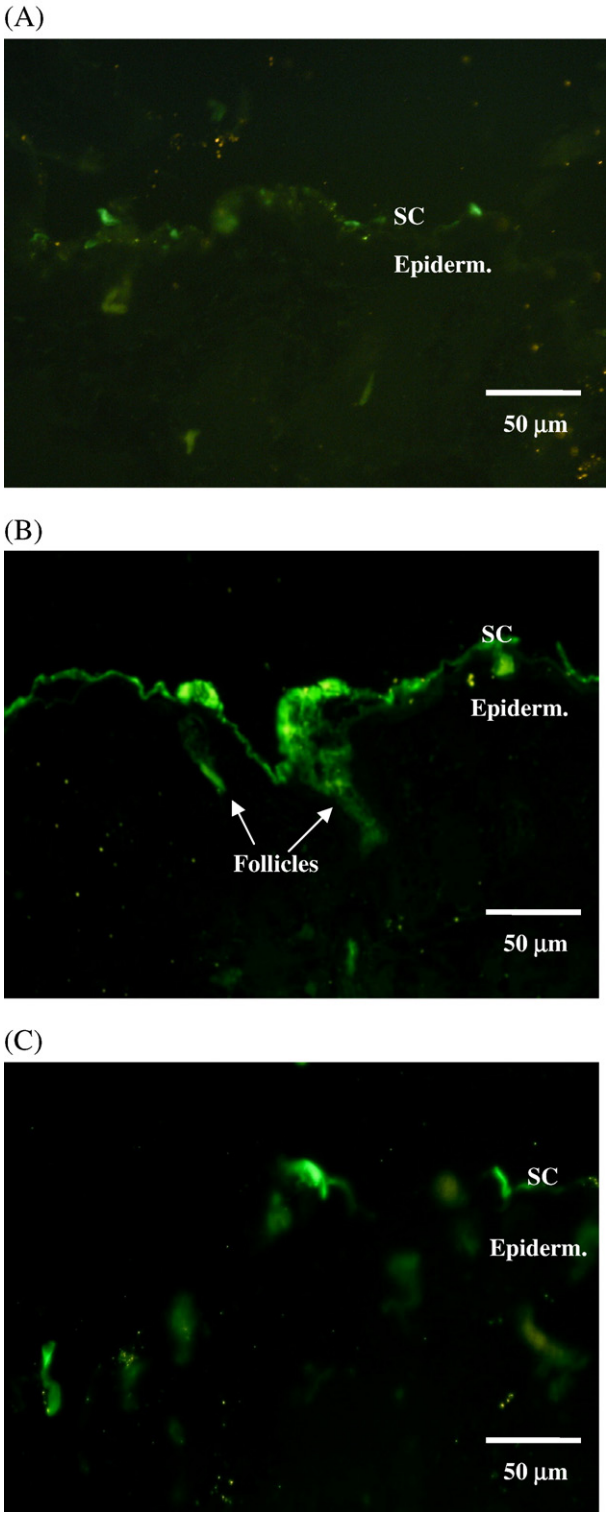

Fig. 2. Fluorescence microscopic examination of nude mouse skin 2 h after in vivo topical administration of a 15-mer ASO to untreated skin (A), 1.4 J/cm^2 laser-treated skin (B), and 1.7 J/cm^2 laser-treated skin (C). (original magnification ×200).

onto the skin. Output energies of 0.35–0.65 J with a beam spot size of 7 mm in diameter could achieve fluences of 0.9–1.7 J/cm^2. The energy of the laser pulse was monitored with an energy meter (Nova Display, Ophir, Israel) before and after treatment.

2.3. In vitro topical administration of ASOs and SRB

The diffusion cell used in this study was a Franz vertical diffusion assembly. A piece of excised nude mouse skin (BALB/c-nu strain, 6–8 weeks old) was mounted on the receptor compartment with the SC side facing upwards into the donor compartment. The laser hand-piece was located approximately 3.7 cm from the skin surface. After laser irradiation, the skin surface was wiped with a cotton wool swab several times. The receptor compartment (5.5 ml) was filled with a pH 7.4 citrate-phosphate buffer. The donor compartment (0.5 ml) contained ASOs (0.43 μM) or SRB (2 mM) in pH 7 buffer and was occluded by paraffin film. The available area of the Franz cell was 1.13 cm^2. The receptor was maintained at 37 °C and stirred by a magnetic bar at 600 rpm. At appropriate intervals, 200-μl aliquots of receptor medium were withdrawn and immediately replaced by an equal volume of fresh medium. The samples taken were measured using a fluorescence spectrometer (F-2500, Hitachi, Tokyo, Japan) at $\lambda_{excitation}$ of 494 nm and $\lambda_{emission}$ of 519 nm for ASOs and $\lambda_{excitation}$ of 560 nm and $\lambda_{emission}$ of 593 nm for SRB.

2.4. Stability of ASOs

The donor and receptor media of ASOs were withdrawn after 36 h of in vitro topical delivery. Samples were analyzed by 1% SDS and 10% PAGE in denaturing conditions, followed by determination with a fluorescence imager (Typhoon 9400, Amersham Biosciences, Buckinghamshire, UK).

2.5. In vivo topical administration of ASOs and SRB

A glass cylinder with an available area of 0.785 cm^2 was attached to the back skin of a female nude mouse with glue. ASOs or SRB in pH 7 buffer (0.2 ml) at a concentration of 0.43 μM or 2 mM respectively was added to each cylinder. The vehicle was applied to the skin with and without laser treatment. The application time of the vehicle was 2 h. After excising the skin on which the vehicle had been applied, the skin was wiped 10 times with a cotton cloth. All procedures were carried out in the dark to prevent the influence of ambient light.

Immediately after treatment, a specimen of ASO-exposed area was taken for examination by fluorescence microscopy. The disc-

Table 2
The fluxes and enhancement ratios of sulforhodamine B across nude mouse skin by treatment of Er:YAG laser

Fluence (J/cm^2)	Original flux (nmol/cm^2/h) [a]	Normalized flux (nmol/cm^2/h) [b]	Enhancement ratio (ER) [c]
0	3.22±0.88	–	–
1.4	16.80±2.96	43.60±7.68	13.5
1.7	16.44±2.62	42.53±6.78	13.2

Each value represents the mean±S.D. (n=4).
[a] Original flux was calculated directly from the flux across partly laser-treated skin.
[b] Normalized flux was calculated from the flux across fully laser-treated skin (100%), which was calibrated by flux of control group (without laser treatment).
[c] Enhancement ratio (ER) was normalized flux of laser-treated group/flux of control group.

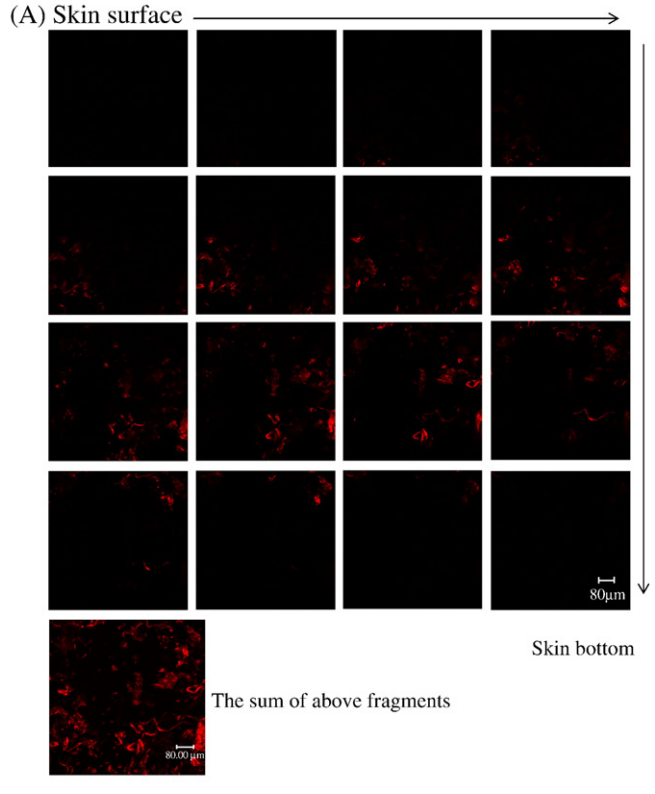

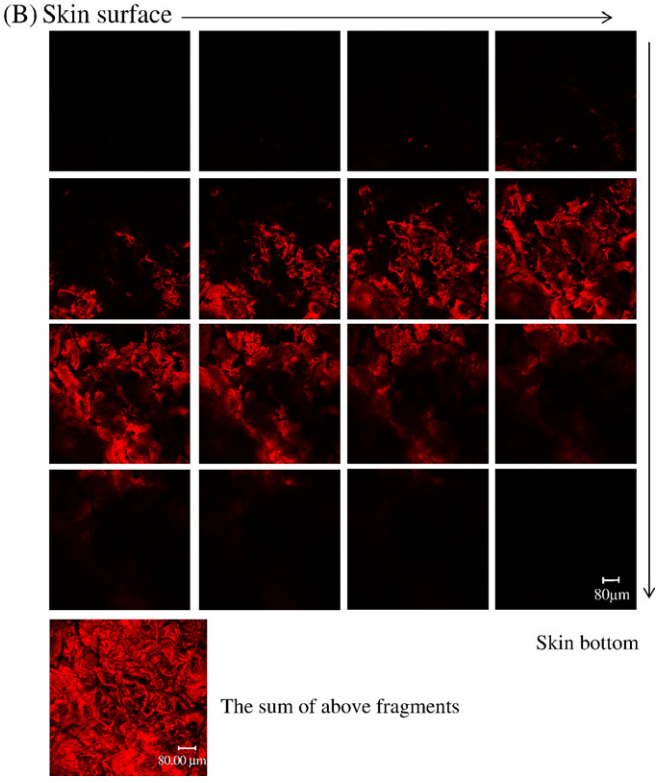

Fig. 3. Confocal laser scanning microscopic (CLSM) micrographs of nude mouse skin after in vivo topical administration of SRB via skin for 2 h on untreated skin (A), 1.4 J/cm^2 laser-treated skin (B), and 1.7 J/cm^2 laser-treated skin (C). (original magnification ×20). The skin specimen was viewed by CLSM at 7–10 μm increments through the *Z*-axis. The arrows indicate the skin fragments from surface to bottom. The images below the photographs of the 16 fragments are the sum of all fragments (full-thickness skin).

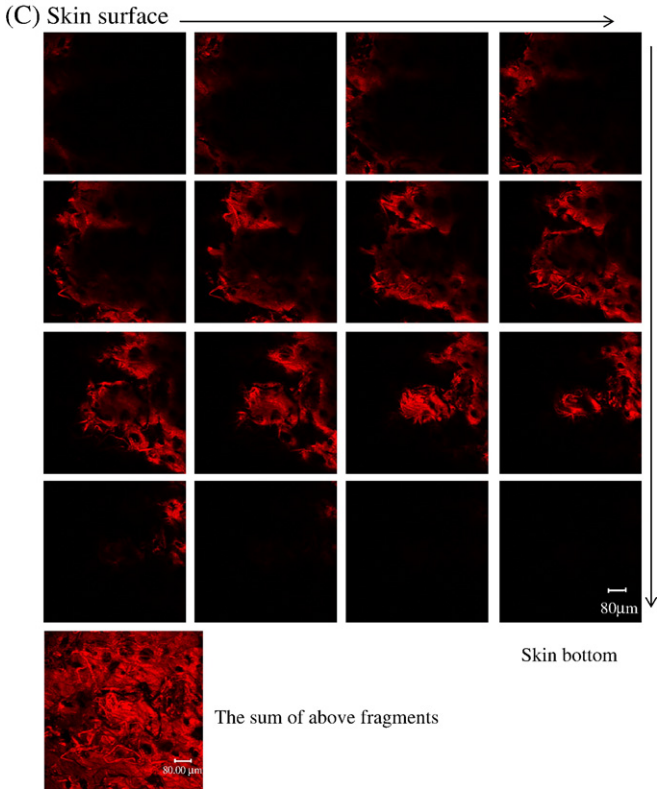

Fig. 3 (*continued*).

shaped biopsies were cut in half along the diameter, embedded in OCT, and frozen in a freezer at −70 °C. Samples were then sectioned in a cryostat microtome. Sections were mounted with glycerin and gelatin. Fluorescence photomicrographs of the sections were obtained with an Olympus BX-51 microscope (Tokyo, Japan) using a filter set having $\lambda_{excitation}$ at 470–490 nm and $\lambda_{emission}$ at 515–700 nm. The SRB-exposed samples were directly examined by confocal laser scanning microscopy (CLSM). The full thickness was optically scanned at 7–10-μm increments through the *Z*-axis of a Leica TCS SP2 confocal microscope (Wetzlar, Germany). Optical excitation was carried out with a 543-nm He–Ne laser beam, and fluorescence emission was detected at 560–620 nm.

2.6. Plasmid DNA amplification

The pCMV-*lac* Z and pAcGFP1-C1 vectors were transformed into *E. coli* (strain DH5-α)-competent cells using standard procedures and then amplified and purified using column chromatography. The purity of the plasmid was measured by OD_{260}/OD_{280} (1.85–1.90; OD, optical density) as well as by electrophoresis in a 0.8% agarose gel. Purified plasmid DNA was resuspended in sterile double-distilled water and frozen in aliquots.

2.7. In vivo plasmid DNA expression in skin

The procedure for in vivo topical administration of plasmid DNAs was the same as for ASO administration. The 1 mg/ml

plasmid DNA in pH 7 citrate-phosphate buffer was used as the vehicle. The duration of administration was 6 h for pCMV-*lac* Z and 4 h for pAcGFP1-C1. Punch biopsies were performed 15 and 24 h after removal of pCMV-*lac* Z and pAcGFP1-C1, respectively.

Expression of β-galactosidase was detected by an X-gal histological assay. The harvested skin samples were immediately fixed in 2% (v/v) formaldehyde–0.2% (v/v) glutaraldehyde in PBS at 25 °C for 8 h. Tissues were then rinsed with PBS three times and incubated in the stained X-gal solution at 37 °C for 10 h. Each specimen was fixed in a 10% buffered formaldehyde solution at pH 7.4 for 2 h. The specimen was cut vertically against the skin surface. Each section was embedded in paraffin wax. For each skin sample, three different sites were examined and evaluated under light microscopy (Nikon Eclipse 4000, Tokyo, Japan). Photomicrographs of the three randomly selected sites of each sample were taken with a digital camera (Nikon Coolpix 900, Tokyo, Japan). Cells transfected with β-galactosidase-expressing plasmid appeared blue following fixation and incubation with the X-gal substrate. The transfected area was quantitatively measured using an image measurement software (SPOT® 4.6, Diagnostic Instruments, MI, USA) The skin sections by the side of the examined sections were stained with hematoxylin and eosin (H&E) for comparison.

For analysis of GFP expression, the CLSM was used to scan the fluorescence signal of GFP at different skin depths. Optical excitation was carried out with a 488-nm argon laser, and the fluorescence emission was detected at 500–535 nm. The fluorescence signal was quantified by Leica Q-Win® software.

2.8. Statistical analysis

The statistical analysis of differences between different treatments was performed using unpaired Student's *t*-test. A 0.05 level of probability was taken as the level of significance.

3. Results

3.1. In vitro topical administration of ASOs

The cumulative amount of ASOs (pmol/cm^2) in the receptor compartment as a function of time after laser treatment along with various energies is shown in Fig. 1. The slopes of the resulting plots were computed, and fluxes (pmol/cm^2/h) were calculated from the slopes (Table 1). ASOs showed very low permeability across the skin without laser treatment. This result may indicate that the SC layer has a more-pronounced barrier effect on ASOs with hydrophilic and multi-charged characteristics. Er:YAG laser exposure above a fluence of 1.2 J/cm^2 of a limited area of the skin surface of ~34% of the permeated area increased the 15-mer ASO permeability ($p<0.05$). On the other hand, the Er:YAG laser was effective in enhancing 25-mer ASO permeation for all intensities studied ($p<0.05$, Table 1). Extrapolating the original flux data of the laser-irradiated area to an area of 100% exposure (normalized flux) resulted in respective permeation enhancement ratios (ERs) of 4.38–29.93 and 4.11–29.16 for 15- and 25-mer ASOs.

The data in Table 1 show that the normalized flux of ASOs across SC-stripped skin was 25–30-fold higher than that across intact skin. The furry BALB/c mouse skin was also used as a barrier in this study since it has a typical and great number of hair follicles. The hair of the skin was shaved before the experiment. The passive flux of a 15-mer ASO across furry mouse skin was 0.50±0.12 pmol/cm^2/h, which was slightly but significantly higher ($p<0.05$) than that across nude mouse skin. The original flux of the 15-mer ASO across furry mouse skin treated with 1.4 J/cm^2 was 6.89±1.84 pmol/cm^2/h. The ER after calibration of the normalized flux was 38.59 in this case.

3.2. In vivo topical administration of ASOs

Fig. 2A shows a fluorescence microscopic photograph from an untreated site (control) of skin with 15-mer ASO absorption. No fluorescence signal was observed in the profiles of skin treated with blank buffer (no ASOs, data not shown). Topical ASO application without laser treatment produced a very slight fluorescence signal in the SC with no evidence of diffusion into the epidermis. As shown in Fig. 2B, it appears that the depth and the efficiency of ASO permeation increased by applying a fluence of 1.4 J/cm^2. The fluorescence signal was able to reach the lower epidermis. A significant signal was observed in the

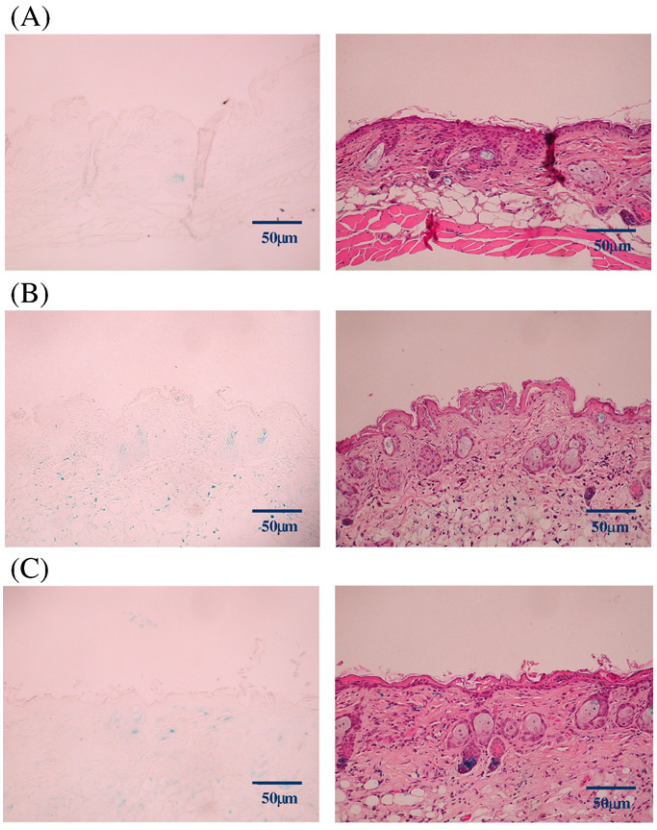

Fig. 4. Expression of β-galactosidase in nude mouse skin 6 h after in vivo topical administration of pCMV-*lac* Z gene to untreated skin (A), 1.4 J/cm^2 laser-treated skin (B), and 1.7 J/cm^2 laser-treated skin (C). (original magnification ×20). The H&E staining photographs (in the right-hand panel) corresponding to the X-gal staining photographs (in the left-hand panel).

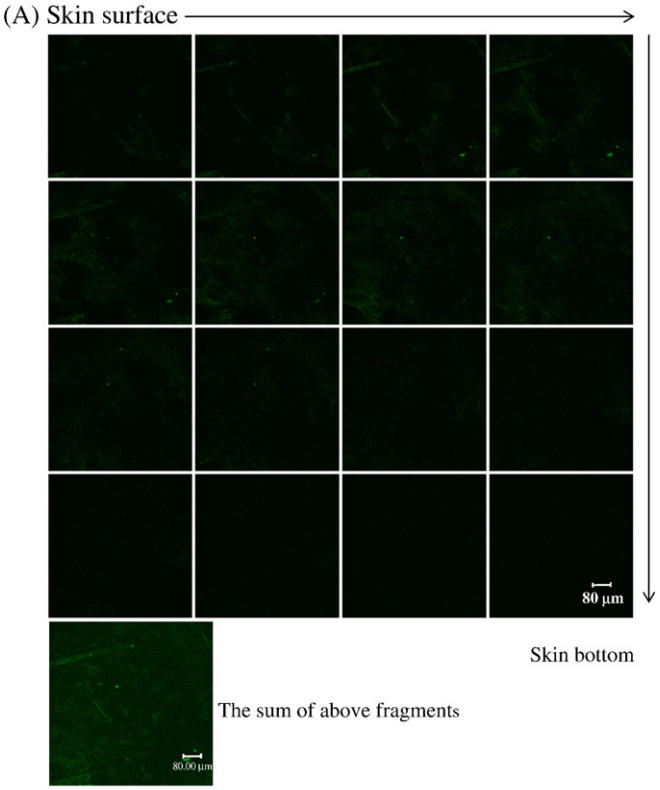

Fig. 5. Confocal laser scanning microscopic (CLSM) micrographs of nude mouse skin after in vivo topical administration of pAcGFP1-C1 via skin for 2 h on untreated skin (A), 1.4 J/cm^2 laser-treated skin (B), and 1.7 J/cm^2 laser-treated skin (C). (original magnification ×20). The skin specimen was viewed by CLSM at 7–10 μm increments through the *Z*-axis. The arrows indicate the skin fragments from surface to bottom. The images below the photographs of the 16 fragments are the sum of all fragments (full-thickness skin).

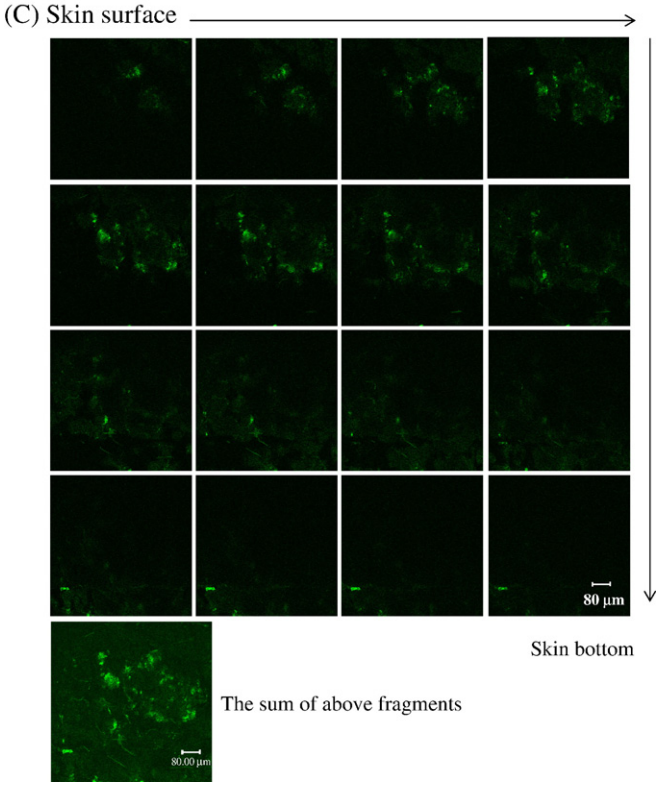

Fig. 5. (*continued*).

hair follicles. In the case of the 1.7 J/cm^2-treated group (Fig. 2C), the intensity of the signal was between that of control group and the 1.4 J/cm^2-treated group. Very few ASOs were found below the SC.

3.3. In vitro and in vivo topical administration of SRB

Whether the pathway of skin permeation was heterogeneous or homogeneous by the laser could be visualized by monitoring permeation of a dye, SRB. Previous study has utilized SRB as a model for investigating the ASO permeation pathway by ultrasound [4]. SRB was administered in vitro to examine the effect of the Er:YAG laser on its permeation. Fluences of 1.4 and 1.7 J/cm^2 were selected in this experiment. As shown in Table 2, the laser significantly promoted ($p<0.05$) SRB delivery via the skin. The ERs by both fluences were comparable, which showed lower values compared to those of ASOs. Fig. 3 shows confocal images obtained from control and laser-treated samples of nude mouse skin after in vivo SRB application. The full skin thickness was optically scanned at 7–10-μm increments for 16 fragments from the surface of skin (left to right, top to bottom). The images below the 16 fragments (larger photographs) are a compilation of these 16 fragments. Since the thicknesses of nude mouse SC and epidermis are ~11 and ~18 μm respectively [12], the first 4 fragments could be characterized as SC and epidermal parts. There was no signal in the group treated with blank buffer (no SRB, data not shown). As shown in Fig. 3A, no or only negligible signals were detected in the SC and epidermis of the untreated group. A

more-significant signal of SRB was observed in the upper and middle dermis. Compared to the control, increased red fluorescence in skin treated with the laser can clearly be seen with the intense signal (Fig. 3B,C). There was almost no signal in the SC and epidermis for a 1.4 J/cm^2-treated skin. On the other hand, some red fluorescence could be detected in the SC and epidermis for the 1.7 J/cm^2-treated group.

3.4. In vivo plasmid DNA expression in skin

To assess the targeting characteristics of gene transfection by the Er:YAG laser, β-galactosidase and GFP expression vectors were delivered to nude mouse skin in vivo. In these experiments, the skin was exposed to laser fluences of 1.4 and 1.7 J/cm^2. As shown in Fig. 4A, there is almost no β-galactosidase expression in the intact skin. A slight blue staining was detected in a hair follicle. However, there was no sign of plasmid DNA diffusion into the epidermis. After a 1.4-J/cm^2 treatment of the Er:YAG laser, extensive expression of the *lac* Z gene was observed in the dermis and subcutis, including the hair follicles. Gene expression was seen in dermal fibroblasts, macrophages, follicular keratinocytes, and epidermal interfollicular keratinocytes (Fig. 4B). Skin depth targeting was achieved by a fluence of 1.4 J/cm^2 on the topically applied *lac* Z gene. DNA penetrated the skin and was effectively expressed in the entire dermis, subcutis, and hair follicles. The 1.7 J/cm^2-treated group showed a weaker blue staining compared to the 1.4 J/cm^2-treated group (Fig. 4C). β-Galactosidase expression was distributed in the upper to lower dermis and hair follicles. The 1.7-J/cm^2 fluence also induced significant β-galactosidase staining compared to the control. The transfected area exposed by 1.4 and 1.7 J/cm^2 showed a 14.0- and 6.8-fold increase as compared to the non-treated group respectively.

Fig. 5A shows the confocal images of GFP expression in intact skin by in vivo topical DNA vector pAcGFP administration. No or only a negligible fluorescence signal was obtained in the entire skin depth. A laser fluence of 1.4 J/cm^2 greatly enhanced the expression of GFP from the SC to the lower dermis (Fig. 5B). Similar to the results for the *lac* Z gene, a fluence of 1.7 J/cm^2 produced a paler signal compared to that of the 1.4-J/cm^2 fluence. The fluorescence signal was quantified by Q-Win® software, and the results are depicted in Table 3. Quantification was performed directly by summing the 16 fragments for each sample. A fluence of 1.4 J/cm^2 enhanced GFP expression of the pAcGFP gene by 164-fold compared to the control.

Table 3
The amounts of fluorescence signal in the images of confocal laser scanning microscopy of nude mouse skin treated with Er:YAG laser after pAcGFP vector administration

Fluence (J/cm^2)	Pixel (light unit) [a]	Enhancement ratio (ER) [b]
0	10,575±2178	–
1.4	1,732,396±233,821	164
1.7	62,235±19,510	6

Each value represents the mean±S.D. (n=4).
[a] Pixel was the amount of fluorescence signal quantified by software.
[b] Enhancement ratio (ER) was pixel of laser-treated group/pixel of control group.

4. Discussion

Two ASOs with 15- and 25-mer lengths were used in this experiment. The 15-mer ASO used here is complementary to a site of the UL52 essential gene of herpes simplex virus-1 [16]. The integrity of the tested ASOs in the donor and receptor compartments was determined after 36 h of contact with the skin. No degradation of ASOs was found in the PAGE analysis (data not shown). This suggests that ASOs remained fairly stable in the skin.

It is clear that the threshold of laser fluence for inducing meaningful enhancement of ASO permeation was lower for the 25-mer ASO (Table 1). This may have been due to the transport of ASOs being inversely related to size [17]. The slight structural alteration in 0.9 J/cm^2-treated skin was not sufficient to alter the possibility of the 15-mer ASO entrance. The more-significant changes in skin structure with the higher laser fluences may generally have led to higher enhancement of ASO permeation. As depicted in our previous studies, the etched thickness of the SC layer after laser ablation appears to be proportional (correlation coefficient, r=0.95) to the treated fluence [11,14].

Three mechanisms, including direct ablation, optical breakdown (photomechanical stress), and rapid heating, are involved in skin structural alterations by laser irradiation [18]. The Er:YAG laser emits light which ablates the SC with a minimal residual thermal effect [19], hence the heating mechanism of this laser can be ignored. Photomechanical stress is produced by broadband compressive waves, which appear to directly interact with cells and tissues [20]. Previous studies suggested that the photomechanical waves induce expansion of the lacunar spaces within the highly tortuous intercellular domains leading to the formation of transient channels [21,22]. These ultrastructural changes of the SC were confirmed for the Er:YAG laser in our previous studies [11,12]. The Er:YAG laser acts on the lipid-rich pathways by photomechanical waves, but also on the intracellular regions by disrupting the corneocytes [15]. Both pathways may contribute to the enhancement of ASO permeation by the Er:YAG laser.

This enhancement of ASO permeation across SC-stripped skin is comparable to that of laser-treated skin by fluences of 1.4–1.7 J/cm^2. Since the Er:YAG laser only partly ablates the SC layer, this confirms that other mechanisms are involved in the ultrastructural alteration of the skin. A morphological study revealed that the hair follicles of nude mouse skin greatly differ from those of the furry mouse [23]. The normalized flux of a 15-mer ASO across furry mouse skin and nude mouse skin treated with a 1.4 J/cm^2 of fluence were respectively 5.91- and 38.59-fold higher than that of the passive control. This may indicate that the follicles play an important role in the laser-mediated enhancement of ASO permeation.

Another observation is that the slopes of in vitro permeation profiles gradually increased with time. This may indicate that the ASO permeation was accelerated at the latter stage of

application. The drug should partition into the SC, then pass across the skin. The partitioning of the drug would be gradually saturated following the increase of time, leading to the sufficient amount for penetrating into receptor. Another reason may be the skin disruption at the latter stage of application. One of the characteristics of an ideal enhancing method is that the skin should recover its normal barrier properties following removal of the enhancing method. Consequently the safety of the laser is crucial for its applicability. The Er:YAG laser tested in this study used lower energies than those utilized in clinical situations for therapeutic aims. As the SC regenerates rapidly, the skin should recover after laser treatment. In our previous studies, the skin recovered to a normal status within 3 days, which was evaluated by the SC thickness and transepidermal water loss [12,14]. The histological observation also showed that only SC ablation and no gross disruption were detected in the epidermis and dermis. Hence although some skin disruption may occur in the in vitro permeation experiment, the in vivo or clinical safety of Er:YAG laser application could be assured.

There was almost no fluorescence signal of ASO in intact skin with in vivo topical administration (Fig. 2A). This is probably a consequence of the lower affinity of the ASOs for the SC and tissue proteins in viable skin [24]. Application of the Er:YAG laser largely increased ASO absorption into the skin reservoir, especially into the hair follicles. Photomechanical waves of lasers show promise for drug delivery at both the organ and cellular level. Photomechanical waves appear to directly interact with cells through mechanical forces [22]. It has been shown that photomechanical waves can permeabilize the plasma membrane and nuclear envelop of the cell and facilitate the delivery of macromolecules into the cell [25,26]. Our previous study also indicated that the Er:YAG laser acts on both intercellular pathways and keratinocytes [11]. Hence the Er:YAG laser may permeabilize skin cells, facilitating intracellular uptake of antisense compounds. However, further study is needed to elucidate this mechanism. The fluorescence of the hair follicles in 1.4 J/cm^2-treated skin suggests that ASO had diffused into the follicles as elucidated by the in vitro administration across furry mouse skin.

Photomechanical stress waves can be characterized as broad-band-pulsed ultrasound [22]. Physical forces such as photomechanical waves and ultrasound target the weaker lipid domains in the SC [21,27]. Ultrasound produces heterogeneous ASO permeation into the skin. Heterogeneous permeation leads to the formation of localized transport pathways [4]. It is of interest to compare the permeabilization pattern produced by photomechanical waves with that by ultrasound. Microscopic observation of the laser-treated skin showed no intensely stained spots on the skin like with ultrasound treatment. The confocal images of laser-treated skin also showed no specific localization of the fluorescence signal. This suggests that photomechanical waves by the Er:YAG laser interact with the skin in ways that are different from those of ultrasound.

Plasmid DNA diffusion to the target tissue is expected to be low because of the low transfection efficiency of plasmids in normal skin [28]. It is important to enhance the transfection of DNAs by external forces. There was almost no β-galactosidase expression in the untreated skin except for a slight blue staining detected in a hair follicle. This suggests that plasmid DNA had diffused into the follicles. The skin treated with a fluence of 1.7 J/cm^2 showed weaker *lac* Z gene expression than did a fluence of 1.4 J/cm^2. This phenomenon was also observed in the in vitro 25-mer ASO permeation and in vivo fluorescence microscopic observation of ASOs. It is generally accepted that higher fluences produce greater ablation and disruption of the SC. The opposite results observed in the present study may have been due to characteristics of the Er:YAG laser on skin tissues. The permeant is first partitioned into the SC, after which it passes across the skin by various pathways. Ablation of the SC layer of the skin reduces the inherent barrier properties of the SC and thus increases the skin permeation; however, partitioning of the permeant into the SC and subsequent diffusion into viable skin may be retarded because of the limited area of the SC after laser ablation [11,14]. As a result, the increased permeation of the skin due to structural alterations may be partly offset by a reduction in partitioning.

Another explanation is that a certain level of water in the SC reduces the rigidity of keratinocytes and thus increases drug diffusion. The Er:YAG laser decreases the water retention in the skin, because this laser emits light with a 2940-nm wavelength which is highly absorbed by water [29]. The water content decreases as the laser energy is increased. This effect is responsible for the ASO and DNA absorption being rather difficult with less water in the skin under occlusion.

A 164-fold increase in GFP expression was detected for Er:YAG laser treatment on the skin at a fluence of 1.4 J/cm^2. The ablative effect and photomechanical stress waves were the main mechanisms enhancing DNA delivery via the skin. SC ablation facilitates DNA transport into the skin. Then photomechanical waves permeabilize cell membranes, thus promoting DNA delivery into the cytoplasm. Previous studies demonstrated that the Nd:YAG laser and titanium-sapphire femtosecond-pulsed laser can increase GFP expression by in vitro gene transfer into mammalian cells [30,31].

The Er:YAG laser maximally increased ASO and DNA permeation by 30- and 160-fold in the present study. Other physical methods for direct gene transfer to skin, including electroporation, gene gun, puncture, ultrasound, and iontophoresis, have recently been reported. Direct SC removal by tape-stripping can increase gene expression primarily in the superficial epidermis and in hair follicles [6]. Plasmid DNA penetration by combining tape-stripping and electroporation, a high voltage pulse, is limited to the superficial layers of the skin, probably due to the large size (4.7 kb) of DNA [2]. This limitation can be overcome by using the Er:YAG laser. Zhang et al. [32] demonstrated a 16-fold increase in the number of transfected skin cells with electroporation compared with the control . The electroporation approach allows depth targeting in follicles and the dermis [33]. A commercially available gene gun (Helios gene gun, Bio-Rad, Hercules, CA, USA) accelerates DNA-coated gold particles into the skin, and gene expression is limited to the upper dermis [5]. Puncture-mediated gene transfer related to tattooing shows a ~8-fold increase in gene expression in both superficial and subepidermal skin

tissues [34]. Ogura et al. [35] assessed the intradermal injection of DNA, followed by irradiation of photomechanical waves by the Nd:YAG laser. β-Galactosidase and GFP were selectively expressed in epidermal cells. The ablation and photomechanical waves induced by the Er:YAG laser may extend the DNA distribution within the skin with no need of an injection. With respect to ASOs, their permeation by electroporation has been extensively investigated. A 2–10-fold of enhancement is achieved depending on the molecular mass and voltage used [16,24,36]. Lin et al. [9] reported that the combination of iontophoresis and microprojection patch technology enhanced the flux of a 20-mer ASO by ~100-fold. The localized transport pathways induced by ultrasound may occupy ~5% of the exposed skin area [4]. The Er:YAG laser may cause a more-equal force on the irradiated skin area as compared to that by ultrasound. It should be noted that the permeation procedures and evaluation methods differed in those investigations. Hence comparisons among various enhancing methods should be cautious.

5. Conclusions

High levels of target gene expression are desirable for producing a biologically significant phenotype in many cutaneous gene therapy approaches. This study showed that the Er:YAG laser can efficiently deliver topically applied ASOs and plasmid DNA into the skin under both in vitro and in vivo conditions. The chief mechanisms of the Er:YAG laser are SC ablation and photomechanical waves. An increase in the laser fluence did not necessary enhance ASO and DNA permeation. Gene partitioning into the skin may have contributed to the mechanism influencing the absorption of ASOs and DNA via the skin. In vivo laser-controlled depth-targeting gene delivery opens a new perspective in the development of skin gene therapy for diseases of the superficial, intermediate, and deep layers of the skin. With the present method, only a single pulse was needed to successfully deliver the studied compounds. In addition, laser treatment did not require contact with tissue, which greatly differs from electroporation, gene gun, and ultrasound transfection.

References

[1] D. Sawamura, X. Meng, S. Ina, H. Ishikawa, K. Tamai, K. Nomura, K. Hanada, I. Hashimoto, Y. Kaneda, In vivo transfer of a foreign gene to keratinocytes using the hemagglutinating virus of Japan-liposome method, J. Invest. Dermatol. 108 (1997) 195–199.

[2] N. Dujardin, P. Van deŕ Smissen, V. Préat, Topical gene transfer into rat skin using electroporation, Pharm. Res. 18 (2001) 61–66.

[3] M. González Ferreiro, L. Tillman, G. Hardee, R. Bodmeier, Characterization of complexes of an antisense oligonucleotide with protamine and poly-L-lysine salts, J. Control. Release 73 (2001) 381–390.

[4] A. Tezel, S. Dokka, S. Kelly, G.F. Hardee, S. Mitragotri, Topical delivery of anti-sense oligonucleotides using low-frequency sonophoresis, Pharm. Res. 21 (2004) 2219–2225.

[5] M.T.S. Lin, L. Pulkkinen, J. Uitto, Cutaneous gene therapy: principles and prospects, Dermatol. Clin. 18 (2000) 177–189.

[6] W.H. Yu, M. Kashani-Sabet, D. Liggitt, D. Moore, T.D. Heath, R.J. Debs, Topical gene delivery to murine skin, J. Invest. Dermatol. 112 (1999) 370–375.

[7] R.M. Brand, P.L. Iversen, Transdermal delivery of antisense compounds, Adv. Drug Deliv. Rev. 44 (2000) 51–57.

[8] N. Raghavachari, W.E. Fahl, Targeted gene delivery to skin cells in vivo: a comparative study of liposomes and polymers as delivery vehicles, J. Pharm. Sci. 91 (2002) 615–622.

[9] W.Q. Lin, M. Cormier, A. Samiee, A. Griffin, B. Johnson, C.L. Teng, G.E. Hardee, P.E. Daddona, Transdermal delivery of antisense oligonucleotides with microprojection patch (Macroflux®) technology, Pharm. Res. 18 (2001) 1789–1793.

[10] J. Hadgraft, Passive enhancement strategies in topical and transdermal drug delivery, Int. J. Pharm. 184 (1999) 1–6.

[11] W.R. Lee, S.C. Shen, H.H. Lai, C.H. Hu, J.Y. Fang, Transdermal drug delivery enhanced and controlled by erbium:YAG laser: a comparative study of lipophilic and hydrophilic drugs, J. Control. Release 75 (2001) 155–166.

[12] W.R. Lee, S.C. Shen, K.H. Wang, C.H. Hu, J.Y. Fang, The effect of laser treatment on skin to enhance and control transdermal delivery of 5-fluorouracil, J. Pharm. Sci. 91 (2002) 1613–1626.

[13] W.R. Lee, S.C. Shen, K.H. Wang, C.H. Hu, J.Y. Fang, Lasers and microdermabrasion enhance and control topical delivery of vitamin C, J. Invest. Dermatol. 121 (2003) 1118–1125.

[14] J.Y. Fang, W.R. Lee, S.C. Shen, Y.P. Fang, C.H. Hu, Enhancement of topical 5-aminolevulinic acid delivery by erbium:YAG laser and microdermabrasion: a comparison to iontophoresis and electroporation, Br. J. Dermatol. 151 (2004) 132–140.

[15] J.Y. Fang, W.R. Lee, S.C. Shen, H.Y. Wang, C.L. Fang, C.H. Hu, Transdermal delivery of macromolecules by erbium:YAG laser, J. Control. Release 100 (2004) 75–85.

[16] V. Regnier, N. De Morre, A. Jadoul, V. Préat, Mechanisms of a phosphorothioate oligonucleotide delivery by skin electroporation, Int. J. Pharm. 184 (1999) 147–156.

[17] R.M. Brand, A. Wahl, P.L. Iversen, Effects of size and sequence on the iontophoretic delivery of oligonucleotides, J. Pharm. Sci. 87 (1998) 49–52.

[18] A.G. Doukas, T.J. Flotte, Physical characteristics and biological effects of laser-induced stress waves, Ultrasound Med. Biol. 22 (1996) 151–164.

[19] R.M.P. Manaloto, T. Alster, Erbium:YAG laser resurfacing for refractory melasma, Dermatol. Surg. 25 (1999) 121–123.

[20] S. Lee, D.J. McAuliffe, T.J. Flotte, N. Kollias, A.G. Doukas, Photomechanical transcutaneous delivery of macromolecules, J. Invest. Dermatol. 111 (1998) 925–929.

[21] G.K. Menon, N. Kollias, A.G. Doukas, Ultrastructural evidence of stratum corneum permeabilization induced by photomechanical waves, J. Invest. Dermatol. 121 (2003) 104–109.

[22] A.G. Doukas, N. Kollias, Transdermal drug delivery with a pressure wave, Adv. Drug Deliv. Rev. 56 (2004) 559–579.

[23] P. Köpf-Maier, V.F. Mboneko, H.J. Merker, Nude mice are not hairless: a morphological study, Acta Anat. 139 (1990) 178–190.

[24] V. Regnier, A. Tahiri, N. André, M. Lemaître, T. Le Doan, V. Préat, Electroporation-mediated delivery of 3′-protected phosphodiester oligodeoxynucleotides to the skin, J. Control. Release 67 (2000) 337–346.

[25] S.E. Mulholland, S. Lee, D.J. McAuliffe, A.G. Doukas, Cell loading with laser-generated stress waves: the role of the stress gradient, Pharm. Res. 16 (1999) 514–518.

[26] T.Y.D. Lin, D.J. McAuliffe, N. Michaud, H. Zhang, S. Lee, A.G. Doukas, T.J. Flotte, Nuclear transport by laser-induced pressure transients, Pharm. Res. 20 (2003) 879–883.

[27] S. Mitragotri, D. Blankschtein, R. Langer, Ultrasound-mediated transdermal protein delivery, Science 269 (1995) 850–853.

[28] D.V. Schaffer, D.A. Lauffenburger, Targeted synthetic gene delivery vectors, Curr. Opin. Mol. Ther. 2 (2000) 155–161.

[29] G. Teikameyer, D. Goldberg, Skin resurfacing with the Er:YAG laser, Dermatol. Surg. 23 (1997) 685–687.

[30] U.K. Tirlapur, K. König, Targeted transfection by femtosecond laser, Nature 418 (2002) 290–291.

[31] M. Terakawa, M. Ogura, S. Sato, H. Wakisaka, H. Ashida, M. Uenoyama, Y. Masaki, M. Obara, Gene transfer into mammalian cells by use of a nanosecond pulsed laser-induced stress wave, Opt. Lett. 29 (2004) 1227–1229.

[32] L. Zhang, L. Li, Z. An, R.M. Hoffman, G.A. Hofmann, In vivo transdermal delivery of large molecules by pressure-mediated electroincorporation and

electroporation: a novel method for drug and gene delivery, Bioelectrochem. Bioenerg. 42 (1997) 283–292.
[33] L. Zhang, L. Li, Z. An, R.M. Hoffman, G.A. Hofmann, Depth-targeted efficient gene delivery and expression in the skin by pulsed electric fields: an approach to gene therapy of skin aging and other diseases, Biochem. Biophys. Res. Commun. 220 (1996) 633–636.
[34] I.F. Ciernik, B.H. Krayenbühl, D.P. Carbone, Puncture-mediated gene transfer to the skin, Hum. Gene Ther. 7 (1996) 893–899.
[35] M. Ogura, S. Sato, K. Nakanishi, M. Uenoyama, T. Kiyozumi, D. Saitoh, T. Ikeda, H. Ashida, M. Obara, In vivo targeted gene transfer in skin by the use of laser-induced stress waves, Lasers Surg. Med. 34 (2004) 242–248.
[36] A.K. Banga, M.R. Prausnitz, Assessing the potential of skin electroporation for the delivery of protein- and gene-based drugs, Trends Biotechnol. 16 (1998) 408–412.